Inorganic Chemistry

Article

pubs.acs.org/IC

Synthesis Mechanism Study of Layered Double Hydroxides Based on Nanoseparation

Zheng Chang,† Caiying Wu,† Sha Song, Yun Kuang, Xiaodong Lei, Liren Wang,* and Xiaoming Sun*

State Key Laboratory of Chemical Resource Engineering, Beijing University of Chemical Technology, Beijing 100029, China

Supporting Information

ABSTRACT: Colloidal layered double hydroxides (LDH) nanosheets were sorted by their lateral sizes using a density gradient ultracentrifuge separation technique. Composition investigations on these size-sorted nanosheets indicated that larger sheets had higher Mg:Al ratio than the smaller ones. Experiments using different Mg:Al feed ratios confirmed that high Mg:Al ratio induced fast sheet growth speed. Tracking the source of the Mg:Al spatial distribution difference in one batch of synthesis at the nucleation process revealed the coprecipitation-redissolution of Mg^{2+}. Thus the discriminative separation of these nanosheets led to a new insight into the structure-composition relationship of LDH nanomaterials and more understanding on their formation mechanism.

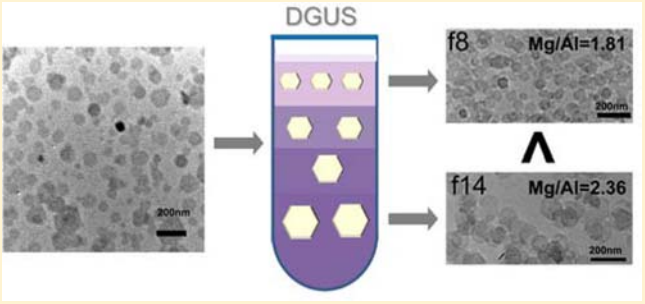

INTRODUCTION

Layered double hydroxides (LDH), also well-known as hydrotalcite-like compounds, are generally formulated as $[M^{II}_{1-x}M^{III}x(OH)_2](A^{n-})x/n{\cdot}mH_2O$ (where M^{II} and M^{III} represent divalent and trivalent metallic ions, respectively; A^{n-}, n-valent anion).[1] Their structure is based on the brucite-like layers, where partial substitution of divalent cations by trivalent ones results in positively charged hydroxide layers, which are balanced by exchangeable interlayer anions.[2] Recently, LDH have received considerable attentions because of their wide applications as catalysts and catalyst supports,[3] absorbents,[4] molecular containers,[5] and other functional materials.[6−8] Various synthesis strategies have been developed for controlling the structure, morphology, and composition of the resulting LDH materials to yield LDH sheets with different particle sizes and compositions.[2,9] Recently, stable homogeneous suspensions of near monodispersed Mg/Al-LDH nanosheets (NSs) in the range of 50−200 nm were made following a modified procedure.[2] A fast coprecipitation of two or more salt solutions under quick mixing with alkali solutions was followed by washing with deionized water to remove excess free ions, and then hydrothermal treatment at a controlled temperature and time. Despite the above-mentioned achievements for the preparation of fairly uniform LDH NSs, small attention has been paid to the relationship between particle size and composition of LDH. It is commonly assumed that the LDH NSs prepared in one batch all have the same composition as long as they are of pure phase, even though they show little size differences. It is natural to consider these in this way since all the sheets from one batch are obtained through the same procedure and under the same conditions. However, another point indicates that the formation of various metallic hydroxides is sequenced in a coprecipitation process, because pH values to induce precipitation of different metal cations are different. For instance, Mg^{2+} commonly precipitates at pH 12, while Al^{3+} precipitates at pH 4, so Al^{3+}-rich LDH should precipitate earlier than Al^{3+}-lean LDH. The difference in crystal seeds' composition might influence structure and composition of terminal LDH although the reactions happen in the same system following the same procedure. This contradiction remains a hypothesis without clear demonstration, nor hard evidence, possibly because of lack of satisfactory separation techniques to sort LDH NSs. Recently, the density gradient ultracentrifugation separation (DGUS) method has been successfully employed in sorting colloidal nanoparticles (e.g., single walled carbon nanotubes,[10,11] Si,[12] and Au nanocrystals[13,14]) according to their size, shape, chemical, and structural differences.[15] Separation on CdS nanorods has inspired us to develop an O_2-manipulated growth method.[16,17]

Herein, we transferred the strategy to investigate the synthesis mechanism of LDH colloids made in one batch. Successfully sorting colloidal Mg/Al-LDH NSs by size using the DGUS method and consequent characterization revealed that the larger LDH NSs exhibited higher Mg:Al mole ratios. It indicated that the lateral growth speed of LDH NSs was affected by their composition even under the same conditions. The deduction was preliminary demonstrated by varying the Mg:Al feed ratio. It also led us to discover 2 stages at the initial nucleation process, including the fast coprecipitation and partial redissolution of Mg^{2+} ions. Finally, a model for LDH NSs formation was proposed.

Received: April 9, 2013
Published: July 23, 2013

ACS Publications © 2013 American Chemical Society

dx.doi.org/10.1021/ic4008763 | Inorg. Chem. 2013, 52, 8694−8698

EXPERIMENTAL DETAILS

Preparation. The targeted Mg/Al-LDH NSs were prepared by coprecipitation and subsequent hydrothermal treatment developed from the literature,[2] in which the salt and alkali solutions were quickly mixed and nucleated in a colloid mill.[18] Typically, for the synthesis of colloidal $Mg_2Al(OH)_6(CO_3)_{1/2}\cdot xH_2O$, 10 mL of mixed salt solution containing $MgCl_2$ (2.0 mmol) and $AlCl_3\cdot 6H_2O$ (1.0 mmol) and 40 mL of NaOH solution (6.0 mmol) were simultaneously poured out into a colloidal mill with vigorous stirring for 10 min (see Supporting Information, Figure S1 for a schematic principle). The resulting slurry was centrifuged at 12,000 rpm for 15 min and washed twice with deionized water to remove the excess free metal salts and alkali, and subsequently dispersed in 40 mL of deionized water. This aqueous suspension was transferred into a stainless steel autoclave with a Teflon lining. The autoclave was then placed in a preheated oven, followed by hydrothermal treatment at 100 °C for 10 h.

Separation. The resulting colloidal suspension was separated by the DGUS method using a five-layer density gradient which was made by aqueous ethylene glycol (EG) solutions with different concentrations (by volume) in a Beckman centrifuge tube (polycarbonate, inner diameter 15 mm, length 90 mm). To make a 20%+40%+60%+80%+100% gradient, 2 mL of 100% EG was added to the centrifuge tube first, then 2 mL of 80% aqueous EG solution was slowly layered above the 100% layer. The subsequent layers were made following the same procedure and resulted in a density gradient along the centrifuge tube. One milliliter of the LDH suspension was layered on top of the gradient prior to ultracentrifugation. The typical ultracentrifugation condition was at 30,000 rpm (relative centrifugal force, RCF = 113600g) for 15 min at 20 °C. Calibrated micropipettors were used to manually extract 500 μL fractions at various positions along the centrifuge tube after ultracentrifugation for characterization.

Characterization. The X-ray powder diffraction (XRD) patterns of the as-prepared samples were recorded on a Shimadzu XRD-6000 power diffractometer using Cu Kα radiation (λ = 1.5418 Å) at 40 kV in the 2θ range of 3−70° with a scanning rate of 10°/min. Transmission electron microscopy (TEM) measurements were conducted on a JEOL JSM-2010 transmission electron microscope equipped with an energy dispersive X-ray spectrometer (EDS) operating at 200 kV. Samples were prepared by ultrasonication in ethanol, and a droplet was dropped onto a carbon-enhanced copper grid. Photon correlation spectroscopy (PCS) was taken on a MALVERN Nanosizer Nano ZS instrument to analyze particle size distribution from 0.6 to 6000 nm. Elemental analysis was performed using a Shimadzu ICP-7500 inductively coupled plasma emission spectrometer. Samples were prepared by dissolving the products in dilute nitric acid at room temperature.

RESULTS AND DISCUSSION

The as-prepared Mg/Al-LDH aqueous suspension was semitransparent and stable even after 3 months, as shown in Figure 1b. The Tyndall effect of the suspension was demonstrated by shining on it with a red LED laser, which suggested the colloids were homogeneous and highly dispersed. The XRD pattern of the powder product collected after centrifugation, washing, and drying is shown in Figure 1a. All of the characteristic diffraction peaks could be clearly indexed to the rhombohedral $Mg_2Al(OH)_6(CO_3)_{1/2}\cdot xH_2O$, in accordance with the standard card JCPDF NO. 35-0965, demonstrating the formation of LDH crystals with high phase purity. The strong intensity of these characteristic peaks revealed a good crystallinity. The TEM image (Figure 1c) indicated the presence of hexagonal nanosheets, as featured for typical LDH crystals, which had a wide lateral size range of 50−200 nm.

Subsequently, the LDH NSs were sorted using the DGUS method based on their size difference. For highly efficient separation of the LDH colloids, choosing an appropriate density gradient media was the first precondition. After

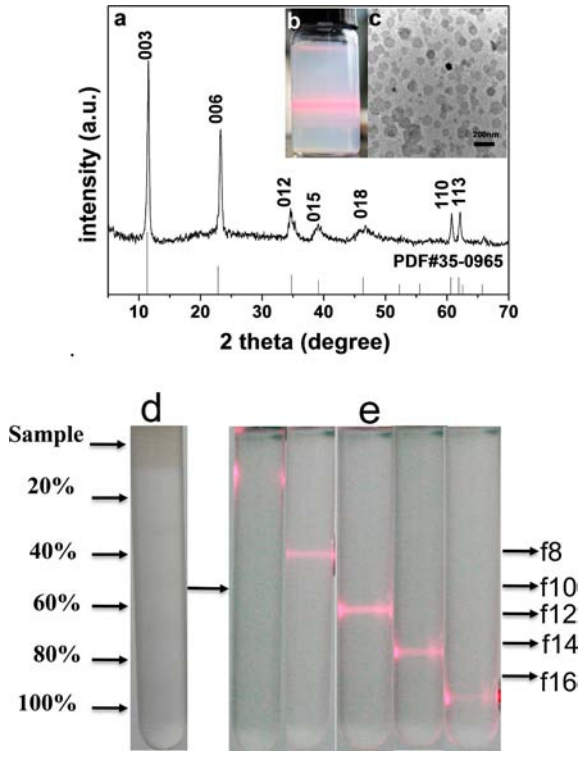

Figure 1. (a) XRD pattern, (b) digital camera image, and (c) TEM image of the as-prepared LDH NSs; digital camera images of the ultracentrifuge tubes before (d) and after (e) DGUS at 30,000 rpm for 15 min.

repeated tests, EG, having a suitable density (1.111 g/cm^3), similar polarity, and high miscibility with water, was chosen to prepare the density gradient, as labeled beside the centrifuge vessel (Figure 1d). After the density gradient ultracentrifugation at 30,000 rpm, the LDH NSs subsided into different zones along the centrifuge tube according to size-dependent sedimentation rates. The Tyndall effect was adopted to identify the locations of LDH NS colloids using a red LED laser from a side (Figure 1e).

The LDH NS fractions were manually sampled out from the very top along the centrifuge tube after ultracentrifugation. TEM images of the typical fractions are shown in Figure 2. It was obvious that the LDH colloids in fraction 8−16 were all sheet-like and nearly monodispersed. The average particle sizes of the separated NSs gradually increased along the centrifuge tube from the top to bottom, indicating that the small NSs sedimented slower than the big ones. It was further confirmed by the statistical size distributions of each fraction measured by counting 100 sheets per fraction, as shown at the right of the corresponding TEM images. But the particle size distributions of fraction 16 and succeeding fractions were relatively wide, possibly related to the thickness increase of NSs. Generally, both the lateral size and thickness of materials have effects on their sedimentation rate. For these thin LDH NSs like those in fraction 8−14, the lateral size was much bigger than the thickness because of the nature of hexagonal LDH NSs, so that the thickness effect was almost ignored and the sedimentation rate was predominantly determined by the lateral size. While for those thick NSs in fraction 16 and succeeding fractions, the thickness effect became as important as the size and consequently made the LDH sheets sediment much faster than those in the upper fractions. In summary, the DGUS

dx.doi.org/10.1021/ic4008763 | Inorg. Chem. 2013, 52, 8694−8698

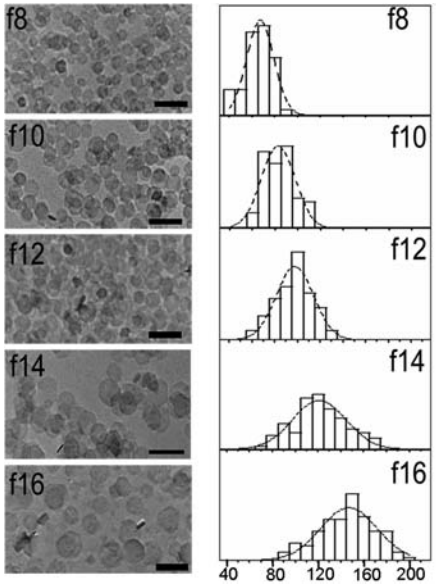

Figure 2. TEM images and statistical size distribution curves of the separated LDH NSs in typical fractions. (The scale bar is 200 nm).

method could successfully sort the colloidal Mg/Al-LDH NSs by size at least for the fractions from f8 to f14.

ICP measurement was carried out on the typical fractions of the LDH NSs to reveal their corresponding compositions. Mg/Al mole ratio and average size of these NSs as a function of fraction number are plotted in Figure 3a. The data of fraction

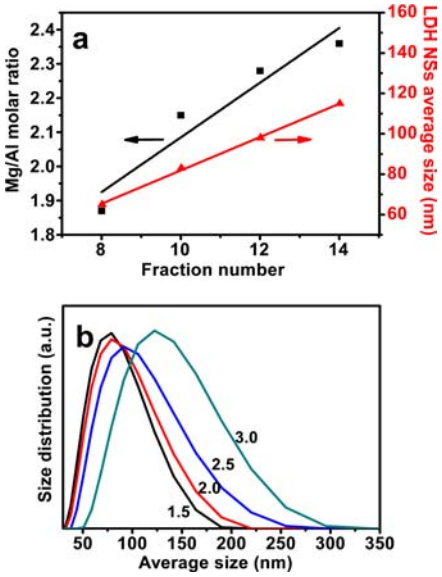

Figure 3. (a) Mg/Al mole ratio (left vertical axis, ■) and average particle size (right vertical axis, ▲) of the separated LDH NSs in different fractions; (b) size distribution curves of the LDH NSs obtained at different Mg/Al feed ratios (1.5, 2.0, 2.5, and 3.0).

16 and following fractions was omitted considering the mixture nature on the lateral size and thickness. Obviously, in fraction 8−14, as the sheet size increased, the Mg/Al ratio of the separated NSs also increased, suggesting Mg content increasing. This indicated that the varied particle size of LDH NSs was closely related to their different composition, even though they were made under the same conditions (e.g., feed ratio, reaction temperature, and time). It denied the previous assumption that the LDH composition in the same system was only determined by the feed ratio as long as they were of pure phase.[19]

The relationship between composition and particle size suggested that the average growth speed of Mg-rich LDH nanosheets was higher than that of Mg-lean ones. If this was right, the LDH NSs obtained at a higher Mg/Al atomic ratio should be bigger in the same reaction time. Therefore, we carried out some experiments to verify it. A series of colloidal LDH NSs were prepared under the same conditions except different feed ratios of magnesium and aluminum salts (Mg/Al = 1.5, 2.0, 2.5 and 3.0, respectively). The particle size distributions of the colloids were measured using dynamic light scattering and are shown in Figure 3b. Indeed it revealed that the average particle size of the LDH NSs gradually increased from 75 to 130 nm when the Mg/Al feed ratio increased from 1.5/1 to 3.0/1. Since all sheets were obtained after the same growth period, a "bigger size" meant a "faster speed", which evidenced our hypothesis that Mg-rich LDH nanosheets grew faster.

Though experimentally evidenced that the faster growth was accompanied with increasing Mg content, it remained an issue how the inhomogeneity of the spatial distribution of the Mg/Al ratio appears at the nucleation stage and affects the growth procedure. To get further insight into the mechanism, we checked the compositions of precipitates and supernatants during a nucleation process with a Mg/Al feed ratio of 3.0/1. After the magnesium and aluminum salt solution and alkali solution were simultaneously added into a colloid mill, the reaction time was recorded as 0 min and then finished in 10 min. The samples were collected in 30 s intervals, and centrifuged to separate the precipitates and supernatants at once. ICP analysis was used to investigate the content evolutions of Mg and Al ions, as plotted in Figure 4. The

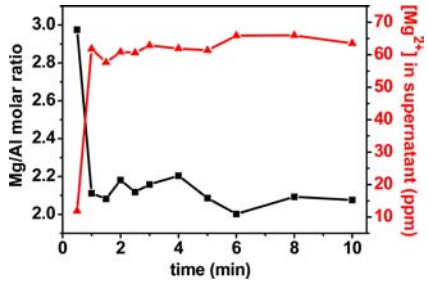

Figure 4. Mg/Al mole ratios (left vertical axis, ■) of the LDH crystal nucleus and Mg concentrations (right vertica axis, ▲) in the supernatants obtained at different reaction times.

detailed data are listed in Supporting Information, Tables S1 and S2. As expected, all the Al ions were completely precipitated as they were always silent in the supernatants. Surprisingly, at the very beginning (0.5 min), the Mg/Al ratio in the precipitate was very high, near to the feed ratio of 3.0/1, and the Mg content in the corresponding supernatant was very low. While at the consequent process (from 1 to 10 min), the Mg/Al ratios in the precipitates sharply decreased and then achieved a platform at Mg/Al = 2.1/1. Meanwhile, the Mg concentrations in the supernatants increased and maintained a high value of ~65 ppm (23 mmol/L), revealing that both Al^{3+} and Mg^{2+} ions originally deposited as precipitates, and then part of the Mg^{2+} ions dissolved again. As we monitored the pH values of the supernatants, they always maintained pH 8−9,

dx.doi.org/10.1021/ic4008763 | Inorg. Chem. 2013, 52, 8694−8698

which suggested that some anions like Cl^- should also have redissolved together with Mg^{2+}, making the pH values unchanged. We believed this might be the origin of the inhomogeneity of the spatial distribution of Mg/Al ratio. It was easily understood that these Mg^{2+} ions, being buried inside the aggregates, would diffuse out slowly, thus keeping higher Mg^{2+} contents, while others near to the surface of the aggregates would reduce Mg^{2+} contents for faster dissolution, which subsequently led to the inhomogeneity of the Mg^{2+} spatial distribution and the different microenvironments for nuclear growth.

On the basis of the above results and the previous reports, we propose a roughly four-stage formation process for the synthesis of Mg/Al-LDH NSs with different particle sizes in the same system, as illustrated in Figure 5. The first stage at 0.5 min corresponded to the coprecipitation of amorphous aluminum hydroxide and magnesium hydroxide once the metallic salts met a strong basic solution in a colloid mill. Because of the very fast precipitation of Mg^{2+} and Al^{3+} ions, Cl^- ions were inevitably precipitated together. In other words, some Mg^{2+} ions in chloride form were absorbed on the precipitates. Subsequently, with the reaction time increasing to 1 min, these magnesium salts redissolved into the solutions to balance the chemical potential of the solution and the solid and to balance the dissolution and precipitation of Mg^{2+} ions at pH 8. The spatial inhomogeneity of the Mg^{2+} ion distribution formed at this stage. The third stage was the formation of the LDH crystal nucleus with different Mg/Al ratios by aluminum atoms diffusing into magnesium hydroxide structures. Finally, the growth/crystallization of the LDH crystal nucleus occurred via a hydrothermal treatment at 100 °C for 10 h. Because of the difference in local Mg^{2+} contents inherited from the crystal nucleus, the crystal growth speeds of LDH NSs varied: when these sheets formed at Mg-rich locations they grew fast while others formed at Mg-lean locations and grew slowly, which led to the presence of LDH NSs with different particle sizes and compositions in the same system.

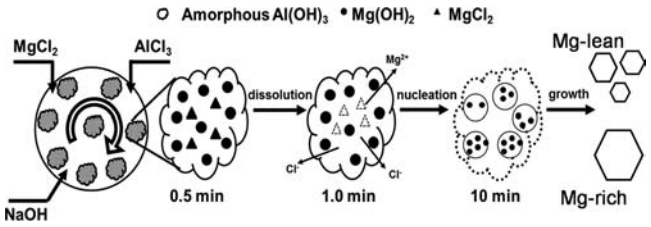

Figure 5. Schematic illustration of a proposed formation mechanism of Mg/Al-LDH NSs with different particle sizes in the same system.

CONCLUSION

In summary, the density gradient ultracentrifugation separation technique has been used for the separation of colloidal LDH NSs prepared in the same batch. TEM analysis demonstrated that the LDH NSs were successfully sorted by their particle sizes. In addition, ICP analysis provided direct information to reveal the relationship between particle size and composition of LDH materials: the particle size increased with the increasing Mg content. According to this structure-composition relationship, we could achieve fine control of the LDH's particle sizes by adjusting the Mg/Al ratio. Finally, the formation procedure of LDH NSs with varied sizes was proposed, which was roughly divided into 4 stages involving coprecipitation of metallic hydroxides and salts, redissolution of magnesium salts, nucleation of LDH, and crystallization of LDH NSs. This demonstrated the potential of extending the DGUS method for the study of structure, composition, and properties of multicomponent nanomaterials.

ASSOCIATED CONTENT

Supporting Information

Further deatils are provided in Figure 1S and Tables 1S and 2S. This material is available free of charge via the Internet at http://pubs.acs.org.

AUTHOR INFORMATION

Corresponding Author

*E-mail: sunxm@mail.buct.edu.cn (X.S.), wanglr@mail.buct.edu.cn (L.W.). Phone: +86-10-64448751. Fax: +86-10-64448751.

Author Contributions

†Contributed equally to this work.

Notes

The authors declare no competing financial interest.

ACKNOWLEDGMENTS

This work was financially supported by the National Natural Science Foundation of China, the 973 Program (2011CBA00503, 2011CB932403), Changjiang Scholars and Innovative Research Team in University (IRT1205).

REFERENCES

(1) Hu, G.; O'Hare, D. *J. Am. Chem. Soc.* **2005**, *127*, 17808−17813.
(2) Xu, Z. P.; Stevenson, G. S.; Lu, C.-Q.; Lu, G. Q. M.; Bartlett, P. F.; Gray, P. P. *J. Am. Chem. Soc.* **2006**, *128*, 36−37.
(3) Feng, J.-T.; Ma, X.-Y.; Evans, D. G.; Li, D.-Q. *Ind. Eng. Chem. Res.* **2011**, *50*, 1947−1954.
(4) Pavan, P. C.; Gomes, G. A.; Valim, J. B. *Microporous Mesoporous Mater.* **1998**, *21*, 659−665.
(5) Wei, M.; Yuan, Q.; Evans, D. G.; Wang, Z.; Duan, X. *J. Mater. Chem.* **2005**, *15*, 1197−1203.
(6) Lou, X. W.; Deng, D.; Lee, J. Y.; Archer, L. A. *J. Mater. Chem.* **2008**, *18*, 4397−4401.
(7) Gursky, J. A.; Blough, S. D.; Luna, C.; Gomez, C.; Luevano, A. N.; Gardner, E. A. *J. Am. Chem. Soc.* **2006**, *128*, 8376−8377.
(8) Khan, A. I.; Lei, L.; J, A.; Norquist; O'Hare, D. *Chem. Commun.* **2001**, 2342−2343.
(9) Yang, Y.; Zhao, X.; Zhu, Y.; Zhang, F. *Chem. Mater.* **2012**, *24*, 81−87.
(10) Green, A. A.; Hersam, M. C. *Mater. Today* **2007**, *10*, 59−60.
(11) Kuang, Y.; Liu, J.; Sun, X. *J. Phys. Chem. C* **2012**, *116*, 24770−24776.
(12) Mastronardi, M. L.; Hennrich, F.; Henderson, E. J.; Maier-Flaig, F.; Blum, C.; Reichenbach, J.; Lemmer, U.; Kübel, C.; Wang, D.; Kappes, M. M.; Ozin, G. A. *J. Am. Chem. Soc.* **2011**, *133*, 11928−11931.
(13) Bai, L.; Ma, X.; Liu, J.; Sun, X.; Zhao, D.; Evans, D. G. *J. Am. Chem. Soc.* **2010**, *132*, 2333−2337.
(14) Li, S.; Chang, Z.; Liu, J.; Bai, L.; Luo, L.; Sun, X. *Nano Res.* **2011**, *8*, 723−728.
(15) Sun, X.; Tabakman, S. M.; Seo, W.-S.; Zhang, L.; Zhang, G.; Sherlock, S.; Bai, L.; Dai, H. *Angew. Chem., Int. Ed.* **2009**, *48*, 939−942.
(16) Sun, X.; Ma, X.; Bai, L.; Liu, J.; Chang, Z.; Evans, D. G.; Duan, X.; Wang, J.; Chiang, J. F. *Nano Res.* **2011**, *4*, 226−232.
(17) Zhang, G.; He, P.; Ma, X.; Kuang, Y.; Liu, J.; Sun, X. *Inorg. Chem.* **2012**, *51*, 1302−1308.
(18) Zhao, Y.; Li, F.; Zhang, R.; Evans, D. G.; Duan, X. *Chem. Mater.* **2002**, *14*, 4286−4291.

(19) Liang, J.; Ma, R.; Iyi, N.; Ebina, Y.; Takada, K.; Sasaki, T. *Chem. Mater.* **2010**, *22*, 371−378.